On the crossover to universal criticality in dilute Ising systems

1995 J. Phys. A: Math. Gen. 28 6073

(http://iopscience.iop.org/0305-4470/28/21/012)

J. Phys. A: Math. Gen. 28 (1995) 6073–6085. Printed in the UK

On the crossover to universal criticality in dilute Ising systems

H K Janssen, K Oerding and E Sengespeick

Institut für Theoretische Physik III, Heinrich-Heine-Universität Düsseldorf, Universitätsstraße 1, 40225 Düsseldorf, Germany

Received 21 March 1995

Abstract. Monte Carlo simulations of the critical behaviour of disordered Ising systems have led to concentration-dependent critical exponents which seem to violate universality. We apply the renormalization group to investigate the crossover effects which cause the observed behaviour. We improve the three-loop expansion of the Callan–Symanzik and Wilson functions by a Padé–Borel approximation and solve the flow equations for various initial points. The exponents found in the simulations can be related to regions in the space of coupling coefficients away from the fixed point.

1. Introduction

Universality is a central feature of critical phenomena. Due to the large correlation length near a critical point the singular behaviour of many thermodynamic observables turns out to be independent of microscopic details of the system. The mathematical description of critical phenomena therefore requires only a small set of relevant and marginal variables.

In this sense the value of the concentration p of magnetic sites in a randomly dilute Ising system should be an irrelevant variable, at least if the impurity density is relatively small and uncorrelated at long distances. Renormalization group calculations [1–3] show that critical exponents and scaling functions are indeed independent of the concentration provided that it is above the percolation threshold p_c and smaller than unity. For concentrations below p_c there is no critical point but only Griffiths singularities [4], whereas for $p = 1$ the system belongs to the universality class of the pure Ising model.

In contrast to this universality, computer simulations of disordered Ising systems at various concentrations produced apparently concentration-dependent exponents [5–8]. This disagreement with the universality predicted by the renormalization group was shown to be induced by a crossover phenomenon which governs a large interval of length scales. Universality only holds in the asymptotic scaling regime of large length and time scales and is not seen in the limited system sizes accessible to simulations. Thus, the simulations show that disordered Ising systems require a considerably larger system size to reach the asymptotic regime than the pure Ising model.

It was argued that the smallness of the crossover exponent ($\phi = \alpha = 0.11$) is responsible for this anomalous behaviour. But this exponent only governs the instability of the Ising fixed point in the renormalization group sense according to the Harris criterion [9]. In principle this exponent has nothing to do with phenomena near the so-called random fixed point which characterizes the universality class of the diluted model. Also it is generally

0305-4470/95/216073+13$19.50

misleading to speak of a crossover from Ising to disordered behaviour. At best what the renormalization group can describe is a crossover from non-universal microscopic behaviour to macroscopic (or mesoscopic) universal phenomena. Sometimes (if the perturbations are small, in our case if p is near unity) this can be described as a crossover between different fixed points. In general, the preasymptotic regime (which is accessible to field theory) has some non-universal aspects. In our opinion this is the origin of the apparent violation of universality in the diluted Ising system. Therefore one has to find out which features of the flow of the (weakly) irrelevant variables under the renormalization group lead to the observed slow crossover.

The field-theoretic formulation of the renormalization group applied to critical phenomena, in general, starts from a semi-microscopic point of view and models the system under consideration by a Hamiltonian constructed from composed fields relevant or weakly irrelevant at least near the upper critical dimension. In the case of our diluted system one assumes that the microscopically uncorrelated elimination of magnetic sites on a lattice can be formulated semi-microscopically as a Gaussian noise (local, and time independent) in the temperature. This is, of course, questionable near the percolation point of the non-magnetic sites but should be correct at lower dilutions. Having formulated the disorder in this way one can show that deviations from Gaussian behaviour are irrelevant (at least near the upper critical dimension). Note that in this argument only the nearly Gaussian character and not the weakness of the disorder is involved. These assumptions lead to a field-theoretic Hamiltonian for the diluted system which has been used for many years [1, 2] and yields flow equations for the coupling constants which have a very special property in the Ising case: they are accidentally degenerate at one-loop order of renormalized perturbation theory. This degeneracy leads to special features: $\sqrt{\epsilon}$-expansions instead of the usual ($\epsilon = 4 - d$)-expansion [2, 3], and a slow crossover of a new form to the trivial fixed point if $d = 4$ [10]. In our opinion it is the shadow of this speciality which is responsible for the slow dilution-dependent crossover in disordered Ising systems also in three dimensions. The underlying physical reason for this degeneracy is so far unknown, although highly interesting.

The paper is organized as follows. In the next section we present the field-theoretic description for an Ising model with random impurities and review its renormalization. We obtain the Wilson functions at three-loop order in a minimal renormalization scheme and solve the renormalization group equation. In section 3 the flow equations for the scale-dependent coupling coefficients are solved in the limit of small $\epsilon = 4 - d$. While this formal limit has no direct physical application it is well suited to elucidate the ideas which motivate the case in section 4 where we consider the three-dimensional model. Using a Padé–Borel approximation to improve the perturbation series for the Wilson functions we calculate the flow of the coupling coefficients for various initial points. For each concentration p considered in [6] we find coupling constants which explain the measured effective exponents. For low dilutions the method applied to identify these coupling constants is directly motivated by the form of the flow. In the last section our results are summarized.

2. The field-theoretic model and its renormalization

As discussed in the first section, in a field-theoretic model the effect of impurities may be described by a local random shift of the temperature. This shift is represented by the Gaussian random field ψ in the Landau–Ginzburg Hamiltonian

$$\mathcal{H}_\psi[s] = \int \mathrm{d}^d r \left[\frac{1}{2}(\tau + \psi)s^2 + \frac{1}{2}(\nabla s)^2 + \frac{1}{4!} g s^4 \right] \tag{1}$$

where s is a one-component order parameter field. For phase transitions with a spontaneously broken O(n)-symmetry ($n \geqslant 2$) the specific heat exponent α is negative (for $d = 3$) and the impurities are irrelevant for the asymptotic critical behaviour [9].

To compute correlation functions we perform the average over ψ at the beginning of the calculation. As usual we introduce n replicas s_α ($\alpha = 1, \ldots, n$) and take the ($n \to 0$)-limit of correlation functions to avoid the problem of ψ-dependent normalization constants [1]. Averaging the Boltzmann weight $\exp(-\sum_{\alpha=1}^{n} \mathcal{H}_\psi[s_\alpha])$ with respect to ψ yields the effective Hamiltonian

$$\mathcal{H}[s] = \int \mathrm{d}^d r \left[\sum_{\alpha=1}^{n} \left(\frac{\tau}{2} s_\alpha^2 + \frac{1}{2} (\nabla s_\alpha)^2 + \frac{g}{4!} s_\alpha^4 \right) - \frac{f}{8} \left(\sum_{\alpha=1}^{n} s_\alpha^2 \right)^2 \right]. \tag{2}$$

Here the coupling coefficient f measures the correlations of the disorder

$$\overline{\psi(r)} = 0 \qquad \overline{\psi(r)\psi(r')} = f\delta(r - r') \tag{3}$$

where the bar denotes the average with respect to disorder. For $g = 0$, $f < 0$ the limit $n \to 0$ of correlation functions calculated with the Hamiltonian (2) has been used to study the statistics of self-avoiding linear polymers.

Due to the singular behaviour of the Gaussian propagator at small distances the perturbative calculation of Green functions (treating the coupling coefficients f and g as perturbations) leads to ultraviolet divergences in the individual terms of the perturbation series. We render these terms finite by analytic continuation in d (dimensional regularization) and absorb the remaining poles in ϵ into renormalizations of coupling coefficients and fields (minimal renormalization). The renormalizations which are necessary to render all static correlation functions free of ϵ-poles are defined by

$$\begin{aligned} s &\to \mathring{s} = Z_s^{1/2} s \qquad & f &\to \mathring{f} = S_d^{-1} (Z_v / Z_s^2) v \mu^\epsilon \\ \tau &\to \mathring{\tau} = (Z_\tau / Z_s) \tau \qquad & g &\to \mathring{g} = S_d^{-1} (Z_u / Z_s^2) u \mu^\epsilon \end{aligned} \tag{4}$$

where μ is an external momentum scale and S_d is the surface area of the d-dimensional unit sphere divided by $(2\pi)^d$.

The integrals which have to be calculated to obtain the Z-factors at three-loop order are the same as in the case of the pure Ising model. One may thus adopt the integrals given in [11] and multiply them with the required n-dependent symmetry factors [12] (see also [13]).

In this paper we also wish to study the critical dynamics of Ising systems with quenched random impurities. In the case of a non-conserved order parameter the dynamics can be expressed in the form of the Langevin equation

$$\partial_t s(r, t) = -\lambda \frac{\delta \mathcal{H}_\psi[s]}{\delta s(r, t)} + \zeta(r, t) \tag{5}$$

where ζ is a Gaussian random force with zero mean and the correlation

$$(\zeta(r, t)\zeta(r', t')) = 2\lambda\delta(r - r')\delta(t - t'). \tag{6}$$

An equivalent formulation is given by the stochastic functional [14–17]

$$\mathcal{J}_\psi[\tilde{s}, s] = \int \mathrm{d}t \int \mathrm{d}^d r \tilde{s} \left(\partial_t s + \lambda \frac{\delta \mathcal{H}_\psi[s]}{\delta s} - \lambda \tilde{s} \right) \tag{7}$$

where $\tilde{s}$ is a response field which has been introduced to average over the thermal noise. Correlation functions and response functions can be calculated as functional integrals with

the weight $\exp(-\mathcal{J}_\psi[\tilde{s}, s])$. Since this weight requires no ψ-dependent normalization constant one may average over disorder without introducing replicas [18]:

$$\overline{\exp(-\mathcal{J}_\psi[\tilde{s}, s])} = \exp(-\mathcal{J}[\tilde{s}, s]) \tag{8}$$

where

$$\mathcal{J}[\tilde{s}, s] = \int \mathrm{d}^d r \left[\int \mathrm{d}t\, \tilde{s}\left(\partial_t s + \lambda(\tau - \Delta)s + \tfrac{1}{6}\lambda g s^3 - \lambda \tilde{s}\right) - \tfrac{1}{2}\lambda^2 f \left(\int \mathrm{d}t\, \tilde{s} s \right)^2 \right]. \tag{9}$$

To render Green functions with different time arguments finite one has to introduce a renormalized response field and a renormalized Onsager coefficient:

$$\tilde{s} \to \mathring{\tilde{s}} = Z_{\tilde{s}}^{1/2} \tilde{s} \qquad \lambda \to \mathring{\lambda} = (Z_s / Z_{\tilde{s}})^{1/2} \lambda . \tag{10}$$

In [12, 19] $Z_{\tilde{s}}$ was calculated by minimal renormalization to two-loop order.

With the required renormalizations at hand we are in a position to derive the renormalization group equation (RGE). The bare Green function

$$\mathring{G}_{\tilde{N},N}(\{r, t\}) = \langle \mathring{\tilde{s}}(r_1, t_1) \ldots \mathring{\tilde{s}}(r_{\tilde{N}}, t_{\tilde{N}}) \mathring{s}(r_{\tilde{N}+1}, t_{\tilde{N}+1}) \ldots \mathring{s}(r_{\tilde{N}+N}, t_{\tilde{N}+N}) \rangle \tag{11}$$

is independent of the momentum scale μ introduced in (4), consequently its derivative at fixed bare parameters vanishes:

$$0 = \mu \left.\frac{\mathrm{d}}{\mathrm{d}\mu}\right|_0 \mathring{G}_{\tilde{N},N} = \mu \left.\frac{\mathrm{d}}{\mathrm{d}\mu}\right|_0 Z_{\tilde{s}}^{\tilde{N}/2} Z_s^{N/2} G_{\tilde{N},N} . \tag{12}$$

Therefore the renormalized Green function $G_{\tilde{N},N}$ satisfies the RGE

$$\left[\mu \frac{\partial}{\partial \mu} + \beta_u \frac{\partial}{\partial u} + \beta_v \frac{\partial}{\partial v} + \kappa_\tau \tau \frac{\partial}{\partial \tau} + \kappa_\lambda \lambda \frac{\partial}{\partial \lambda} + \tilde{N}\tilde{\eta}/2 + N\eta/2 \right] \times G_{\tilde{N},N}(\{r, t\}; \tau, \lambda, u, v; \mu, L) = 0 \tag{13}$$

with the Callan–Symanzik functions

$$\beta_u(u, v) = \mu \left.\frac{\mathrm{d}}{\mathrm{d}\mu}\right|_0 u \qquad \beta_v(u, v) = \mu \left.\frac{\mathrm{d}}{\mathrm{d}\mu}\right|_0 v \tag{14}$$

and the Wilson functions

$$\begin{aligned} \tilde{\eta}(u, v) &= \mu \left.\frac{\mathrm{d}}{\mathrm{d}\mu}\right|_0 \ln Z_{\tilde{s}} & \kappa_\tau(u, v) &= \frac{1}{\tau}\mu \left.\frac{\mathrm{d}}{\mathrm{d}\mu}\right|_0 \tau \\ \eta(u, v) &= \mu \left.\frac{\mathrm{d}}{\mathrm{d}\mu}\right|_0 \ln Z_s & \kappa_\lambda(u, v) &= \frac{1}{\lambda}\mu \left.\frac{\mathrm{d}}{\mathrm{d}\mu}\right|_0 \lambda . \end{aligned} \tag{15}$$

In equation (13) the last argument L of the Green function denotes the linear size of the system.

At three-loop order we have

$$\begin{aligned} \beta_u(u, v)/u = {} & -\epsilon + \tfrac{3}{2}u - 6v - \tfrac{17}{12}u^2 + \tfrac{23}{2}uv - \tfrac{41}{2}v^2 + \left(\tfrac{145}{64} + \tfrac{3}{2}\zeta(3)\right)u^3 \\ & - \left(\tfrac{393}{16} + 18\zeta(3)\right)u^2 v + \left(\tfrac{2925}{32} + 72\zeta(3)\right)uv^2 - \left(\tfrac{821}{8} + 84\zeta(3)\right)v^3 \end{aligned} \tag{16}$$

(here ζ is a Riemann ζ-function),

$$\begin{aligned} \beta_v(u, v)/v = {} & -\epsilon + u - 4v - \tfrac{5}{12}u^2 + \tfrac{11}{2}uv - \tfrac{21}{2}v^2 + \tfrac{7}{8}u^3 \\ & - \left(\tfrac{321}{32} + 3\zeta(3)\right)u^2 v + \left(\tfrac{659}{16} + 24\zeta(3)\right)uv^2 - \left(\tfrac{185}{4} + 33\zeta(3)\right)v^3 \end{aligned} \tag{17}$$

$$\eta(u, v) = \tfrac{1}{24}u^2 - \tfrac{1}{4}uv + \tfrac{1}{4}v^2 - \tfrac{1}{64}u^3 + \tfrac{9}{64}u^2 v - \tfrac{3}{8}uv^2 + \tfrac{1}{4}v^3 \tag{18}$$

and

$$\kappa_\tau(u,v) = \tfrac{1}{2}u - v - \tfrac{5}{24}u^2 + \tfrac{5}{4}uv - \tfrac{5}{4}v^2 + \tfrac{7}{16}u^3 - \tfrac{251}{64}u^2v + \tfrac{333}{32}uv^2 - \tfrac{111}{16}v^3 . \tag{19}$$

At two-loop order the dynamic Wilson function κ_λ is given by

$$\kappa_\lambda(u,v) = v + \tfrac{1}{24}\left(6\ln\tfrac{4}{3} - 1\right)u^2 - \tfrac{1}{4}uv + \tfrac{5}{4}v^2 . \tag{20}$$

No three-loop calculation has been performed as yet. Only for the pure Ising model the three-loop contribution to κ_λ was calculated in [20] with the result .

$$\kappa_\lambda(u,0)/\eta(u,0) = \left(6\ln\tfrac{4}{3} - 1\right) - \frac{3}{4}\left[(3 - 13\ln 4 + 21\ln 3)\ln\tfrac{4}{3} - \pi^2 + 8\int_{1/4}^{1} \mathrm{d}t\,\frac{\ln t}{t-1}\right]u . \tag{21}$$

The general solution of the RGE (13) may be written in the form

$$\begin{aligned} &G_{\tilde{N},N}(\{r,t\};\tau,\lambda,u,v;\mu,L) \\ &\quad = \tilde{X}(l)^{\tilde{N}/2}X(l)^{N/2}G_{\tilde{N},N}(\{r,t\};Y_\tau(l)\tau,Y_\lambda(l)\lambda,\bar{u}(l),\bar{v}(l);\mu l,L) \\ &\quad = (\tilde{X}(l)l^{d+2})^{\tilde{N}/2}(X(l)l^{d-2})^{N/2} \\ &\qquad \times G_{\tilde{N},N}(\{lr,Y_\lambda(l)l^2t\};Y_\tau(l)l^{-2}\tau,\lambda,\bar{u}(l),\bar{v}(l);\mu,lL) \end{aligned} \tag{22}$$

where the last equality follows from dimensional analysis, and the characteristics are solutions of the ordinary differential equations

$$\begin{aligned} &l\frac{\mathrm{d}}{\mathrm{d}l}\ln\tilde{X}(l) = \tilde{\eta}(\bar{u}(l),\bar{v}(l)) \qquad l\frac{\mathrm{d}}{\mathrm{d}l}\ln X(l) = \eta(\bar{u}(l),\bar{v}(l)) \\ &l\frac{\mathrm{d}}{\mathrm{d}l}\ln Y_\tau(l) = \kappa_\tau(\bar{u}(l),\bar{v}(l)) \qquad l\frac{\mathrm{d}}{\mathrm{d}l}\ln Y_\lambda(l) = \kappa_\lambda(\bar{u}(l),\bar{v}(l)) \\ &l\frac{\mathrm{d}}{\mathrm{d}l}\bar{u}(l) = \beta_u(\bar{u}(l),\bar{v}(l)) \qquad l\frac{\mathrm{d}}{\mathrm{d}l}\bar{v}(l) = \beta_v(\bar{u}(l),\bar{v}(l)) \\ &\tilde{X}(1) = X(1) = Y_\tau(1) = Y_\lambda(1) = 1 \qquad \bar{u}(1) = u \qquad \bar{v}(1) = v . \end{aligned} \tag{23}$$

For small l equation (22) maps the large length and time scales of the critical region on scales on which Green functions may be calculated perturbatively. In this limit the scale-dependent coupling constants $\bar{u}(l)$ and $\bar{v}(l)$ approach a fixed point (u_*, v_*), and the characteristics are asymptotically proportional to powers of l. In this way critical exponents can be identified as Wilson functions at the fixed point.

3. Crossover in 3.99 dimensions

As already mentioned in the introduction, the renormalization group transformation possesses no infrared-stable fixed point of order ϵ. This peculiarity of the dilute Ising model is due to the degeneracy of the one-loop contributions to β_u and β_v (equations (16), (17)): both are proportional to $(u-4v)$. The appropriate procedure in this case was found by Khmelnitskii who introduced a $\sqrt{\epsilon}$-expansion to study the critical behaviour of disordered Ising systems [2].

To explain the special property of the flow equations, which in our opinion slows down the crossover, we now consider a diluted version of the 'imaginary' system introduced some time ago by Wilson and Fisher [21]. We set, for example, $\epsilon = \frac{1}{100}$ and study the flow for a system in 3.99 spatial dimensions. For such a small ϵ we have of course $\epsilon \ll \sqrt{\epsilon}$. We

represent the renormalized coupling constants as $u = Aw^3$, $v = \frac{1}{4}Aw^2$, and find the flow equations as an expansion with respect to the amplitude A

$$\frac{\mathrm{d}\ln w}{\mathrm{d}t} = \tfrac{1}{2}A(1-w)w^2 + \mathrm{O}(A^2) \tag{24}$$

$$\frac{\mathrm{d}\ln A}{\mathrm{d}t} = \epsilon - A^2\left(\tfrac{19}{12}w^2 - \tfrac{13}{8}w + \tfrac{19}{32}\right)w^4 + \mathrm{O}(A^3)\,. \tag{25}$$

Here we have set $l = \exp(-t)$. Equations (24) and (25) yield the well known fixed point $w_* = 1 + \mathrm{O}(\sqrt{\epsilon})$, $A_* = \sqrt{96\epsilon/53} + \mathrm{O}(\epsilon)$. We assume that the flow is driven in a first (microscopic) period in a region around this stable fixed point, thus $A \ll 1$. It is easily shown that neglecting the third-order terms of the amplitude A in (25) consistently forces neglect of the second-order terms in (24). For $\epsilon \neq 0$, a possible amplitude scaling is $A \sim \sqrt{\epsilon}$. The two equations (24) and (25) now exhibit a characteristic two-'time' scale behaviour: whereas the modulation w evolves on a 'fast' scale $\sim A^{-1}$ or $\epsilon^{-1/2}$, the amplitude A itself varies on the 'slow' scale $\sim A^{-2}$ or ϵ^{-1}, respectively. Note that this decoupling of A from the fast evolution has its origin in the degeneracy of the one-loop terms in the functions β_u and β_v. The solution of (24) is given by

$$w^{-1} + \frac{w^{-2}}{2} + \ln\left|1 - w^{-1}\right| + \text{constant} = -\frac{1}{2}\int_0^t \mathrm{d}t' A(t') \approx -\frac{A_0}{2}t\,. \tag{26}$$

The last approximation holds for $t \approx \sqrt{\epsilon}^{-1} \ll \epsilon^{-1}$. Such a time is sufficient to drive w practically to one. Thus we have the following flow picture: starting from an initial point (A_0, w_0), the motion goes relatively fast along the trajectory $A \approx A_0$ ($v \sim u^{2/3}$), to the line $w = 1$ ($v = u/4$). After that, a relatively slow motion on this 'fixed point' line sets in. On this line the equation of motion for the amplitude A reads

$$\frac{\mathrm{d}\ln A}{\mathrm{d}t} = \epsilon - \frac{53}{96}A^2 \tag{27}$$

with the solution

$$A = \sqrt{\frac{96\epsilon/53}{1 + \left(96\epsilon/53A_0^{-2} - 1\right)\exp(-2\epsilon t)}}\,. \tag{28}$$

For $t \to \infty$ this slow motion leads to the fixed point $A_* = \sqrt{96\epsilon/53}$. But for a finite system the integration of the flow equations has to finish at $t \sim \ln L$, where L is a suitably scaled measure of the system size. Then $A(\ln L)$ retains information on the initial point through the constant $A_0 = 64v_0^3/u_0^2$ which leads to a residual dilution dependence. For relatively small systems it may occur that the slow motion has not yet set on, and we have $A(\ln L) \approx A_0$. Instead of the true fixed point A_* one has to deal with the (dilution-dependent) quasi-fixed point A_0. As a result one finds effective dilution-dependent exponents. In general, the system sizes used in simulations are not big enough to allow the flow to come sufficiently close to the fixed point. Thus one observes a crossover which depends on the dilution p through A_0. Note that by the clear distinction between the fast and the slow motion, the full information on the initial point (u_0, v_0) is reduced to only one variable $A_0(p)$ after an initial 'time' period which corresponds to small systems.

The anomalous dependence of the amplitude A on the system size especially arises for $\epsilon = 0$. If w is already near one, we obtain

$$|w - 1| = \text{constant} \times \exp\left(-\sqrt{\tfrac{48}{53}\ln L + \left(\tfrac{48}{53}A_0^{-1}\right)^2}\right) \tag{29}$$

$$A = \frac{1}{\sqrt{A_0^{-2} + \frac{53}{48}\ln L}}. \tag{30}$$

The dependence on $\sqrt{\ln L}$ instead of $\ln L$ shows the prolonged crossover to the trivial fixed point. This anomalous dependence has its parallel in the anomalous logarithmic corrections to scaling in dimension four [10].

4. Crossover phenomena

As already pointed out in section 2 asymptotic scaling behaviour with universal critical exponents can only be observed in the limit of large length and time scales. In computer simulations the approach to the scaling regime is mainly limited by the linear size L of the system. Finite-size scaling [22, 23] is valid only in the limit $\xi \to \infty$ (ξ: bulk correlation length) and $L \to \infty$ with ξ/L arbitrary, whereas in computer simulations L is limited by the available CPU time, etc. From the renormalization group point of view the flow parameter l is not sufficiently small (it is of the order $1/L$) in the experiments by Heuer [6, 7] to allow an observation of the asymptotic critical behaviour. We therefore have to solve the flow equations for $\bar{u}(l)$ and $\bar{v}(l)$ with initial coupling coefficients (u, v) different from their fixed point values and study the variation of the Wilson functions along the trajectory of the flow.

To obtain more reliable results we have improved the perturbation series by a modified Padé–Borel approximation of the form

$$F(u,v) = \int_0^\infty \mathrm{d}x \frac{\sum_{k=0}^{3}(\sum_{i=0}^{k} a_{i,k-i}u^i v^{k-i})x^{k+b}}{1+(b_{10}u + b_{01}v)x} \mathrm{e}^{-x} \tag{31}$$

for $F = \beta_u$, β_v, ν, and γ, where $\nu(u,v) = 1/(2 - \kappa_\tau(u,v))$ and $\gamma(u,v) = \nu(u,v)(2 - \eta(u,v))$. Since the three-loop expansion of F is not sufficient to determine all coefficients a_{ij} and b_{ij} in (31) one has to invoke an additional criterion to fix two coefficients and the exponent b. The large-order behaviour of the perturbation theory suggests the same values $b_{10} = \frac{1}{2}$ and $b_{01} = -\frac{3}{2}$ for all functions $F(u,v)$. To see this consider the perturbation series of the β-function of the pure $O(n)$-symmetric ϕ^4-field theory [24]:

$$\beta(u) = \sum_K \beta_K u^K \tag{32}$$

where

$$\beta_K = K!a^K K^{\tilde{b}} c(1 + O(1/K)) \qquad a = -\tfrac{1}{2} \qquad \tilde{b} = 3 + n/2 \tag{33}$$

($n = 1$ for the Ising model). The same constant a as in (33) occurs in the large-order behaviour of the perturbation series of the Wilson functions $\nu(u)$, $\gamma(u)$, etc. For $b_{10} = -a = \frac{1}{2}$, $b = \frac{7}{2}$ the expansion of $F(u,0)$ in powers of u shows the same large-order behaviour as $\beta(u)$.

Since the case $u = 0$, $v < 0$ corresponds to the excluded volume problem ($n = 0$) we set $b = 3$ in the Padé–Borel approximation for $\beta_v(u,v)$. The coefficient $b_{01} = 3a = -\frac{3}{2}$ results from the different normalization of the coupling coefficients f and g in the Hamiltonian (2). To calculate the critical exponents γ and ν we have applied a Padé–Borel approximation for $\gamma(u,v)$ and $\nu(u,v)$ with $b = 0$. In table 1 the exponents obtained in this way are compared with results given in the literature.

Some solutions of the flow equations (23) are depicted in figure 1 together with the fixed point of the pure (I) and the random (R) Ising model. Near the random fixed point

Table 1. Critical exponents of the pure and the disordered Ising model. The exponents of the pure Ising model in the first line were calculated by methods of summation based on Borel transformation and conformal mapping [25]. The exponents of the disordered Ising model in the third line were obtained by a four-loop calculation in $d = 3$ with a [3/1] Padé–Borel approximation [26]. The exponents in the second and fourth lines are computed by the Padé–Borel approximation (31) described in the text.

	γ	ν	β	α
Pure Ising model				
LeG and Z-J	1.241(2)	0.6300(15)	0.3250(15)	0.1100(45)
Padé–Borel (32)	1.251	0.635	0.327	0.095
Dilute Ising model				
Four loop	1.321	0.6714	0.348	−0.013
Padé–Borel (32)	1.313	0.666	0.342	0.002

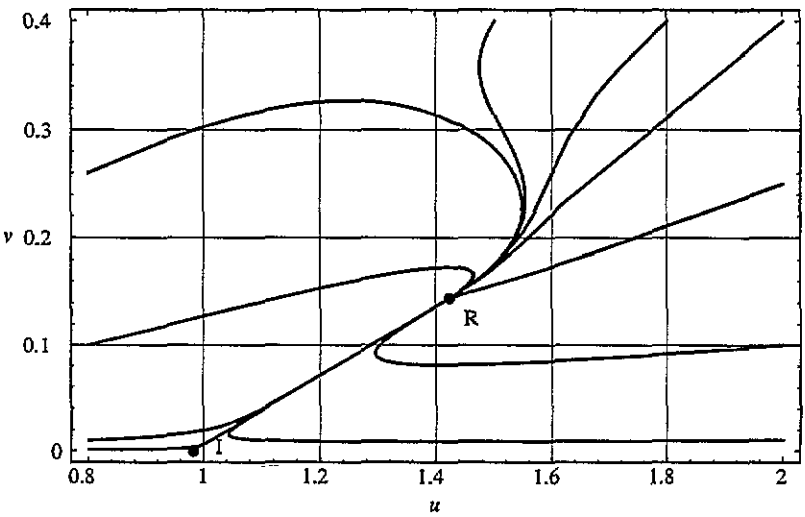

Figure 1. The flow of the coupling constants for various initial points. I denotes the fixed point of the pure Ising model and R indicates the infrared stable disorder fixed point.

the flow may be characterized by the eigenvalues (λ_1, λ_2) and eigenvectors (w_1, w_2) of the stability matrix

$$\begin{pmatrix} \partial_u \beta_u(u,v)|_R & \partial_v \beta_u(u,v)|_R \\ \partial_u \beta_v(u,v)|_R & \partial_v \beta_v(u,v)|_R \end{pmatrix}.$$

With the Padé–Borel approximation (31) for the Callan–Symanzik functions β_u and β_v we obtain

$$\lambda_1 = 0.365\,603 \qquad w_1 = (0.951\,61, 0.307\,309)^{\mathsf{T}} \tag{34}$$

$$\lambda_2 = 0.768\,855 \qquad w_2 = (0.988\,237, 0.152\,928)^{\mathsf{T}}. \tag{35}$$

The eigenvector w_1 (which belongs to the smaller eigenvalue λ_1) defines the direction from which the flow approaches the fixed point at the final stage of the crossover. The point R is reached in the limit $l \to 0$ for all initial coupling constants $u, v > 0$. For small v the trajectory first approaches the unstable manifold of the Ising fixed point and then changes its direction towards the random fixed point. In this range one may speak of a crossover

from Ising to random behaviour. In a strict continuum field theory the flow approaches the line I–R from the left since for $v = 0$ all the range $0 \leqslant \mathring{g} < \infty$ is mapped to the interval $0 \leqslant u < u_I^*$ by the minimal renormalization scheme. However, to explain the sign of the corrections to scaling observed in pure Ising systems one has to apply the RGE in the region of coupling coefficients above the fixed point, i.e. $u > u_I^*$ [27]. This can be justified by a finite lattice spacing Λ^{-1} which allows an approach to the fixed point from above [28, 29]. Applying these considerations to the random Ising model we expect that due to the finite lattice spacing in the simulations the flow approaches the unstable manifold of the Ising fixed point from the right.

We explain the crossover phenomena observed at low dilutions by the two different stages of the flow $(\bar{u}(l), \bar{v}(l))$: in the simulations the effective couplings have already reached the line that connects the two fixed points but not the stable fixed point R. At this point it is helpful to remember the 3.99-dimensional case discussed in section 3 where the modulation w evolves rapidly to its fixed point value w_* while the amplitude A requires a very large 'time' $t = \ln(1/l)$ to come close to A_*. In this picture the line I–R corresponds to a part of the manifold defined by the equation $w(u, v) = w_*$.

Table 2. Effective critical exponents calculated from the Wilson functions $\nu(u, v)$, $\gamma(u, v)$, and $z(u, v)$ compared with results of computer simulations.

	Calculation					Simulation		
p	u_{eff}	v_{eff}	ν	γ	z	ν	γ	z
1.0	0.982	0	0.635	1.251	2.029	0.624(10)	1.22(2)	2.085(10)
0.95	1.182	0.066	0.648	1.277	2.094	0.64(2)	1.28(3)	2.15(1)
0.9	1.375	0.128	0.662	1.306	2.162	0.65(2)	1.31(3)	2.23(1)
0.8	1.647	0.216	0.684	1.351	2.268	0.68(2)	1.35(3)	2.39(1)
0.6	2.353	0.444	0.755	1.501	2.597	0.72(2)	1.51(3)	2.92(2)

To check this assumption more quantitatively we have studied the Wilson functions $\nu(u, v)$ and $\gamma(u, v)$ along the line I–R. It is possible to identify points on this line which reproduce the exponents ν and γ obtained in the simulations at $p = 0.95$ and 0.9 within the bounds of the experimental accuracy (see table 2). The dynamic exponents $z(u, v) = 2 + \kappa_\lambda(u, v)$ calculated in this way are clearly smaller than the values obtained by Heuer [7]. Even for the pure Ising model the exponent z obtained by the same Monte Carlo method is larger than the value predicted by dynamic field theory [30]. The reason for this disagreement is not clear. Note that the most reliable values for z are in agreement with the field-theoretic predictions based on (21) (see [31] and references therein). On the other hand, since the Wilson function κ_λ is known only at two-loop order we expect our approximations to be less accurate for z than for ν and γ. At the random fixed point we find $z = 2.180$. The naive $\sqrt{\epsilon}$-expansion yields

$$\begin{aligned} z &= 2 + \sqrt{\frac{6\epsilon}{53}} + \left(48 \ln \tfrac{4}{3} - \tfrac{1585}{53} - \tfrac{756}{53}\zeta(3)\right)\frac{\epsilon}{106} + \mathcal{O}(\epsilon^{3/2}) \\ &= 2 + 0.336\sqrt{\epsilon}(1 - 0.932\sqrt{\epsilon}) + \mathcal{O}(\epsilon^{3/2}) \end{aligned} \tag{36}$$

(with the three-dimensional estimate $z = 2.023$) while a two-loop calculation in $d = 3$ yields $z = 2.237$ [32].

The effective exponents measured at higher dilutions ($p = 0.6$ and 0.8) cannot be related to points on the unstable manifold of the pure Ising fixed point since they require larger

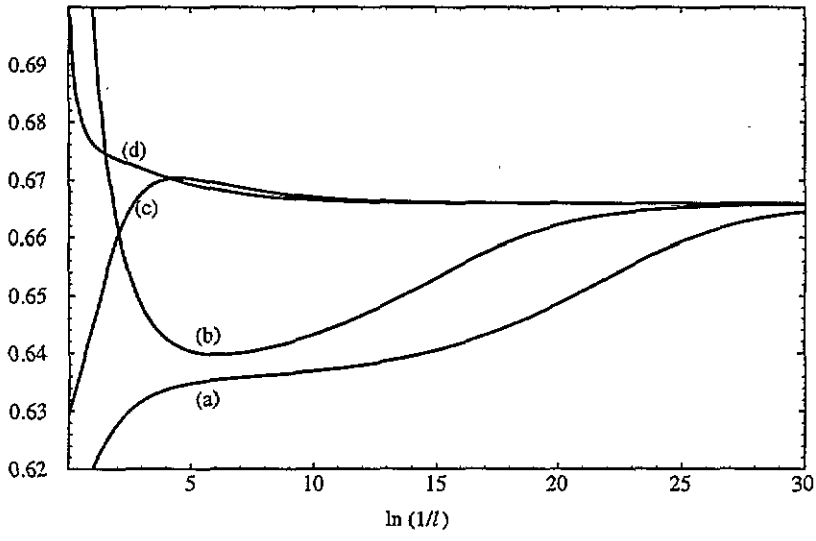

Figure 2. The Wilson function $\nu(\bar{u}(l), \bar{v}(l))$ for initial coupling constants (a) $(u, v) = (0.8, 0.001)$, (b) $(u, v) = (2, 0.01)$, (c) $(u, v) = (1.5, 0.4)$ and (d) $(u, v) = (2, 0.4)$. The curves (a) and (b) correspond to trajectories which approach the line I–R from different directions. Therefore they differ for large $\ln(1/l)$ (when the trajectories have reached the line I–R) only by a shift parallel to the abscissa.

coupling coefficients v. Close to the random fixed point almost all trajectories run along the line

$$(u(t), v(t)) = (u_*, v_*) + t w_1^{\mathsf{T}} \tag{37}$$

where w_1 is the vector defined in (34). It is therefore natural to look for the observed exponents on this line. The coupling coefficients $(u_{\text{eff}}, v_{\text{eff}})$ given in table 2 for $p = 0.8$ and $p = 0.6$ are obtained by minimizing the squared deviations from the experimental results, i.e.

$$a_\nu(\nu(u(t), v(t)) - \nu_{\text{exp}})^2 + a_\gamma(\gamma(u(t), v(t)) - \gamma_{\text{exp}})^2 + a_z(z(u(t), v(t)) - z_{\text{exp}})^2 \tag{38}$$

with $a_\nu = a_\gamma = 1$ and $a_z = 0.01$. We have chosen the weight a_z much smaller than a_ν and a_γ to reduce the influence of the function $z(u, v)$ which is known only to two-loop order. Although the coupling constants $(u_{\text{eff}}, v_{\text{eff}})$ obtained by the minimization of (38) are far away from the fixed point (especially for $p = 0.6$) the exponents ν and γ agree surprisingly well with the experimental values.

In figure 2 the Wilson function $\nu(\bar{u}(l), \bar{v}(l))$ is shown for various initial coupling coefficients using a logarithmic scale for the flow parameter l. In Monte Carlo simulations only a relatively small range of flow parameters can be investigated. The range of system sizes $L = 20 \ldots 60$ studied in [6] corresponds to an interval of length $\Delta \ln(1/l) = \ln 3 \approx 1.1$ in figure 2.

We conclude this section with a discussion of the size dependence of relaxation times. In [7] the relaxation time of the absolute value $\mathcal{M} = |M|$ of the magnetization was measured to obtain the effective dynamic exponents shown in table 2 The integrated relaxation time is defined by

$$T_{\mathcal{M}} = \int_0^\infty \mathrm{d}t \frac{\langle(\mathcal{M}(t) - \langle\mathcal{M}(t)\rangle)(\mathcal{M}(0) - \langle\mathcal{M}(0)\rangle)\rangle}{\langle(\mathcal{M}(0) - \langle\mathcal{M}(0)\rangle)^2\rangle} \tag{39}$$

and satisfies the RGE

$$\left[\mu\frac{\partial}{\partial\mu}+\beta_u\frac{\partial}{\partial u}+\beta_v\frac{\partial}{\partial v}+\kappa_\tau\tau\frac{\partial}{\partial\tau}+\kappa_\lambda\lambda\frac{\partial}{\partial\lambda}\right]T_{\mathcal{M}}(\tau,u,v,\lambda;\mu,L)\,. \tag{40}$$

Solving this equation by the method of characteristics and performing a dimensional analysis one can easily show that

$$T_{\mathcal{M}}(\tau,u,v,\lambda;\mu,L)=l^{-2}(\lambda Y_\lambda(l))^{-1}T_{\mathcal{M}}(Y_\tau(l)l^{-2}\tau,\bar{u}(l),\bar{v}(l);1,\mu,lL)\,. \tag{41}$$

We choose the flow parameter $l=L_0/L$ (where L_0 is some given system size) to obtain at the critical point $\tau=0$

$$T_{\mathcal{M}}(0,u,v,\lambda;\mu,L)=(L/L_0)^2(\lambda Y_\lambda(L_0/L))^{-1}T_{\mathcal{M}}(0,\bar{u}(L_0/L),\bar{v}(L_0/L);1,\mu,L_0)\,. \tag{42}$$

The function $T_{\mathcal{M}}$ can be calculated at leading order in $\epsilon^{1/4}$ by the methods used in [23] to compute the relaxation time spectra. If the ratio L/L_0 is not considerably larger than unity the L dependence of the relaxation time is dominated by the characteristic Y_λ, which may be written as an integral over κ_λ,

$$Y_\lambda(l)=\exp\left(-\int_l^1\frac{\mathrm{d}l'}{l'}\kappa_\lambda(\bar{u}(l'),\bar{v}(l'))\right). \tag{43}$$

For the range of system sizes investigated in the simulations one may use the approximation $\kappa_\lambda(\bar{u}(l),\bar{v}(l))\approx\kappa_\lambda(u_{\mathrm{eff}},v_{\mathrm{eff}})$, where $u_{\mathrm{eff}}\approx\bar{u}(1)$ and $v_{\mathrm{eff}}\approx\bar{v}(1)$, to arrive at the effective power law

$$T_{\mathcal{M}}(L)\approx T_{\mathcal{M}}(L_0)(L/L_0)^{z_{\mathrm{eff}}}\qquad z_{\mathrm{eff}}=2+\kappa_\lambda(u_{\mathrm{eff}},v_{\mathrm{eff}})\,. \tag{44}$$

The simulations show that this approximation is justified for $L_0=20\leqslant L\leqslant 60$ (see [7], figure 3).

5. Summary and outlook

The study of randomly diluted Ising systems by computer simulations has shown the importance of crossover phenomena for the critical behaviour of these systems. The critical exponents found in the simulations depend on the concentration p of magnetic sites while renormalization group calculations predict universal exponents. In this paper we have shown how the observed crossover effects can be explained in the framework of the renormalization group.

While the universal critical exponents correspond to an infrared stable fixed point of the flow equations, the dilution-dependent exponents occur in experiments in which the relevant length or time scales are not sufficiently large to enter the asymptotic scaling regime. This suggests describing the results of the simulations by coupling constants different from their fixed point values. For each concentration $p=0.95, 0.9, 0.8$ and 0.6 we have found coupling coefficients which reproduce the effective exponents ν and γ obtained by Heuer [6] with satisfactory accuracy. For this purpose a Padé–Borel approximation has been used to improve the three-loop expansions of the Callan–Symanzik and Wilson functions. Unfortunately the Wilson function $\kappa_\lambda(u,v)$ which is necessary to calculate the exponent z is known only at two-loop level. This may explain the disagreement between the calculated and measured values for z.

While the goal of this paper was the explanation of crossover phenomena which have already been observed in computer experiments one may also use the effective coupling coefficients $(u_{\mathrm{eff}},v_{\mathrm{eff}})$ to predict the outcome of future experiments. In a subsequent publication we will study the non-equilibrium critical relaxation of dilute Ising systems

from an initial state with short-range correlations. The relaxation process is governed by a new universal exponent θ' [17, 33] which can be calculated by renormalization group methods. We expect that Monte Carlo simulations of the relaxation will be affected by crossover phenomena leading to non-asymptotic (dilution-dependent) exponents θ'.

Acknowledgments

We would like to thank St Theiss for a critical reading of the manuscript. This work was supported by Sonderforschungsbereich 237 (Unordnung und große Fluktuationen) of the Deutsche Forschungsgemeinschaft.

References

[1] Grinstein G and Luther A 1976 Application of the renormalization group to phase transitions in disordered systems *Phys. Rev.* B **13** 1329–43
Lubensky T C 1975 Critical properties of random-spin models from the ϵ-expansion *Phys. Rev.* B **11** 3573–80
[2] Khmelnitskii D E 1975 Second order phase transition in inhomogeneous bodies *Sov. Phys.–JETP* **41** 981–4
[3] Jayaprakash C and Katz H J 1977 Higher-order corrections to the $\epsilon^{1/2}$ expansion of the critical behaviour of the random Ising system *Phys. Rev.* B **16** 3987–90
[4] Griffiths R B 1969 Nonanalytic behaviour above the critical point in a random Ising ferromagnet *Phys. Rev. Lett.* **23** 17–9
[5] Heuer H-O 1990 Monte Carlo simulation of strongly disordered Ising ferromagnets *Phys. Rev.* B **42** 6476–84
[6] Heuer H-O 1993 Critical crossover phenomena in disordered Ising systems *J. Phys. A: Math. Gen.* **26** L333–9
[7] Heuer H-O 1993 Dynamic scaling of disordered Ising systems *J. Phys. A: Math. Gen.* **26** L341–6
[8] Prudnikov V V and Vakilov A N 1993 Computer modeling of the critical dynamics of dilute magnetic materials *Sov. Phys.–JETP* **76** 469–72
[9] Harris A B 1974 Effect of random defects on the critical behaviour of Ising models *J. Phys. C: Solid State Phys.* **7** 1671–92
Harris A B and Lubensky T C 1974 Renormalization-group approach to the critical behaviour of random-spin models *Phys. Rev. Lett.* **33** 1540–43
[10] Geldart D J W and De'Bell K 1993 Logarithmic corrections for dilute uniaxial ferromagnets at the critical dimension *J. Stat. Phys.* **73** 409–14
[11] Brézin E, Le Guillou J C and Zinn-Justin J 1976 Field theoretical approach to critical phenomena, *Phase Transitions and Critical Phenomena* vol 6 ed C Domb and M S Green (New York: Academic) pp 125–247
[12] Sengespeick E 1994 Feldtheorie des kritischen Verhaltens von ungeordneten Ising-systemen *Diploma Thesis* Düsseldorf
[13] De'Bell K and Geldart D J W 1985 Coefficients to $O(\epsilon^3)$ for the mixed fixed point of the nm-component field model *Phys. Rev.* B **32** 4763–5
[14] Janssen H. K 1976 On a Lagrangean for classical field dynamics and renormalization group calculations of dynamical properties *Z. Phys.* B **23** 377–80
De Dominicis C 1976 Techniques de renormalisation de la théorie des champs et dynamique des phénomènes critiques *J. Physique* C **1** 247–53
[15] Bausch R, Janssen H K and Wagner H 1976 Renormalized field theory of critical dynamics *Z. Phys.* B **24** 113–27
[16] De Dominicis C and Peliti L 1978 Field-theory renormalization and critical dynamics above T_c: helium, antiferromagnets, and liquid–gas systems *Phys. Rev.* B **18** 353–76
[17] Janssen H K 1992 On the renormalized field theory of nonlinear critical relaxation *From Phase Transitions to Chaos, Topics in Modern Statistical Physics* ed G Györgyi, I Kondor, L Sasvári and T Tél (Singapore: World Scientific) pp 68–91
[18] De Dominicis C 1978 Dynamics as a substitute for replicas in systems with quenched random impurities *Phys. Rev.* B **18** 4913–19
[19] Lawrie I D and Prudnikov V V 1984 Static and dynamic properties of systems with extended defects: two-loop approximation *J. Phys. C: Solid State Phys.* **17** 1655–68
[20] Antonov N V and Vasilev A N 1985 Critical dynamics as a field theory *Theor. Math. Phys.* **60** 671–9
Janssen H K unpublished
[21] Wilson K G and Fisher M E 1972 Critical exponents in 3.99 dimensions *Phys. Rev. Lett.* **28** 240–3

[22] Fisher M E 1971 The theory of critical point singularities *Critical Phenomena, Proc. 51st Enrico Fermi Summer School* ed M S Green (New York: Academic) pp 1–99
[23] Oerding K 1995 Relaxation times in a finite Ising system with random impurities *J. Stat. Phys.* **78** 893–916
[24] Brézin E, Le Guillou J C and Zinn-Justin J 1977 Perturbation theory at large order. I. The ϕ^{2N} interaction *Phys. Rev.* D **15** 1544–57
[25] Le Guillou J C and Zinn-Justin J 1980 Critical exponents from field theory *Phys. Rev.* B **21** 3976–98
[26] Mayer I O 1989 Critical exponents of the dilute Ising model from four-loop expansions *J. Phys. A: Math. Gen.* **22** 2815–23
Holovatch Yu and Shpot M 1992 Critical exponents of random Ising-like systems in general dimensions *J. Stat. Phys.* **66** 867–83
[27] Liu A J and Fisher M E 1990 On the corrections to scaling in three-dimensional Ising models *J. Stat. Phys.* **58** 431–42
[28] Schäfer L 1994 On the sign of correction to scaling amplitudes: field theoretic considerations and results for self repelling walks *Preprint*
[29] Bagnuls C and Bervillier C 1990 Field-theoretical approach to critical phenomena *Phys. Rev.* B **41** 402–6
Bagnuls C and Bervillier C 1994 Describing actual critical behaviour from field theory: a delicate matter *Phys. Lett.* **195A** 163–70
[30] Heuer H-O 1993 Critical dynamics of the three-dimensional Ising model: A Monte Carlo study *J. Stat. Phys.* **72** 789–827
[31] Grassberger P 1994 Damage spreading and critical exponents for 'model A' Ising dynamics *Preprint*
[32] Prudnikov V V and Vakilov A N 1992 Critical dynamics of dilute magnetic materials *Sov. Phys.–JETP* **74** 990–4
[33] Kissner J G 1992 Nonequilibrium critical relaxation in the presence of random impurities *Phys. Rev.* B **46** 2676–85